

Conductance of a STM contact on the surface of a thin film

N. V. Khotkevych, Yu. A. Kolesnichenko, and J. M. van Ruitenbeek

Citation: *Low Temp. Phys.* **38**, 503 (2012); doi: 10.1063/1.4723673

View online: <http://dx.doi.org/10.1063/1.4723673>

View Table of Contents: <http://ltp.aip.org/resource/1/LTPHEG/v38/i6>

Published by the [American Institute of Physics](#).

Related Articles

First-principles study of electronic structures and photocatalytic activity of low-Miller-index surfaces of ZnO
J. Appl. Phys. **113**, 034903 (2013)

Local ultra-violet surface photovoltage spectroscopy of single thread dislocations in gallium nitrides by Kelvin probe force microscopy
Appl. Phys. Lett. **101**, 252107 (2012)

Temperature dependence of reversible switch-memory in electron field emission from ultrananocrystalline diamond
Appl. Phys. Lett. **101**, 173116 (2012)

Investigation of the conduction in an implanted layer of protons in a potassium lithium tantalate niobate substrate
Appl. Phys. Lett. **101**, 141111 (2012)

Transport properties of surface electrons in helium on a structured substrate
Low Temp. Phys. **38**, 915 (2012)

Additional information on *Low Temp. Phys.*

Journal Homepage: <http://ltp.aip.org/>

Journal Information: http://ltp.aip.org/about/about_the_journal

Top downloads: http://ltp.aip.org/features/most_downloaded

Information for Authors: <http://ltp.aip.org/authors>

ADVERTISEMENT

**AIP**Advances

Submit Now

**Explore AIP's new
open-access journal**

- **Article-level metrics
now available**
- **Join the conversation!
Rate & comment on articles**

ELECTRONIC PROPERTIES OF CONDUCTING SYSTEMS

Conductance of a STM contact on the surface of a thin film

N. V. Khotkevych^{a)} and Yu. A. Kolesnichenko

B. Verkin Institute for Low Temperature Physics and Engineering of the National Academy of Sciences of Ukraine, 47 Lenin Ave., Kharkov 61103, Ukraine

J. M. van Ruitenbeek

Kamerlingh Onnes Laboratorium, Universiteit Leiden, Postbus 9504, 2300 Leiden, The Netherlands

(Submitted January 12, 2012)

Fiz. Nizk. Temp. **38**, 644–652 (June 2012)

The conductance of a contact with a radius smaller than the Fermi wave length was investigated theoretically on the surface of a thin metal film. It is shown that quantization of the electron energy spectrum in the film leads to a step-like dependence of differential conductance $G(V)$ as a function of applied bias eV . The distance between neighboring steps in eV equals the energy level spacing due to size quantization. We demonstrate that a study of $G(V)$ for both positive and negative voltages maps the spectrum of energy levels above and below the Fermi surface in scanning tunneling experiments. © 2012 American Institute of Physics. [<http://dx.doi.org/10.1063/1.4723673>]

1. Introduction

A fairly large number of papers have addressed the problem of calculating point-contact conductance for the analysis and interpretation of results of scanning tunneling microscopy (STM) experiments (e.g., see reviews^{1,2}). The problem of low symmetry and the wide variety of objects under study make the development of a general theory of STM unlikely, and each specific problem is approached differently. Theoretical papers on this subject can be divided into two groups. In one the methods that take into account the specific atomic structure of the STM tip and of the test specimen are used primarily. These methods make it possible to reproduce the crystal structure of the sample surface in calculated STM images, which is very useful for correct interpretation of experimental data. The main deficiency of this approach is the lack of analytical formulas for the STM current–voltage characteristics, since numerical calculations must be performed for every specific case. The other group of works exploits simplified models of noninteracting electrons that allow us to find relatively simple analytical expressions that describe the STM current qualitatively. For this reason such theoretical results are widely used by experimentalists.

One of the first free-electron models describing STM experiments was proposed by Tersoff and Hamann,³ whose theoretical analysis of tunnel current is based on Bardeen's formalism,⁴ in which a tunneling matrix element is expressed by means of independent wavefunctions for the tip and the sample within the barrier region. Using the model wavefunctions the authors³ showed that the conductance of the system is proportional to the local density of states of the sample at the tip position. In principle, it is possible to extract information on subsurface objects (single defects, clusters, interfaces, etc.) by STM, but this requires a more detailed theoretical analysis,⁵ which takes into account the influence of subsurface electron scattering on the tunneling current.

In the physical picture of electron tunneling through a classically forbidden region the electron flow emerging from

the barrier is defined by the agreement between the wavefunctions of carriers incident to the barrier and those transmitted. In a three-dimensional STM geometry the wavefunctions for electrons transmitted through the vacuum region are radically different from the electron wave functions in an isolated sample, and they describe the electron propagation into the bulk from a small region on the surface below the STM tip. In contrast, the theory described in Ref. 3 and its varieties (see Refs. 1 and 2 and references therein) uses unperturbed wavefunctions of the surface Bloch states. Changes in the wavefunctions of transmitted electrons due to scattering by subsurface objects provide information about such scattering in the STM conductance.

The authors of Ref. 6 proposed to introduce the model by Kulik *et al.*⁷ into the theory of STM. In this model a three-dimensional STM tip is replaced with an inhomogeneous barrier in an otherwise nonconducting interface that separates the two conductors. In Ref. 7 it was shown that under the assumption of small transparency of the tunnel barrier the wave function (and thus the current–voltage characteristics) can be found analytically for a tunnel area of arbitrary size. The results for the conductance of the tunnel point contact in Ref. 6 were generalized to an arbitrary Fermi surface for the charge carriers in Refs. 8 and 9. In a series of papers the model described in Ref. 7 has been expanded to describe oscillations of STM conductance resulting from electron scattering due to subsurface defects^{6,8–11} (for reviews see Ref. 12).

Scanning tunneling microscopes have been widely used for the study of various small-sized objects: islands, thin films deposited on bulk substrates, etc.^{13–20} First, a discrete periodic spatial variation of STM current originating from the quantization of electron states was observed in the quantum wedge: a nanoscale flat-top Pb island on a stepped Si(111) surface.¹³ Later the authors showed that the lattice structure of the interface buried under a film of Pb, whose thickness can be as many as 10 times the Fermi wavelength, can be clearly imaged with STM.¹⁴ They concluded that the key to the

transparency of a metal lies in the highly anisotropic motion of electrons and the strong quantization of their transverse wavefunction components. In Ref. 15 the electronic states of thin Ag films grown on GaAs(110) surfaces were investigated by STM with a single layer thickness resolution, and the quantum-well states arising from the confinement geometry of the Ag films were identified. Quantum size effects, that manifested themselves in the formation of new electronically bound states, were investigated by STM on thin islands of Pb of varying heights on the Si(111)-(7×7) surface.¹⁶ It was experimentally demonstrated that scanning tunneling microscopy and spectroscopy of epitaxial Pb islands on Si(111) reveal adiabatic lateral modulation of the energy spectra of the quantum well, providing remote electronic images of the sub-surface reflection phase.¹⁷ In Ref. 18 a step structure was identified at the buried Pb-on-Si(111) 6×6-Au interface by utilizing the quantum well states. It was demonstrated that the spatial step positions, as well as step heights, can be extracted nondestructively and with atomic layer precision by STM. Vertical Friedel oscillations in interface-induced surface charge modulations of Pb islands of a few atomic layers on the incommensurate Si(111)-Pb surface have been observed.¹⁹ Thus, detailed experimental results have been obtained, but a microscopic theory for STM tunneling spectra on samples of finite size has not been reported, which provides the motivation for the present work. Current-voltage characteristics for size quantization in planar thin film geometries of metal-insulator-metal tunneling junctions have been investigated theoretically.^{21,22} Standing electron wave states in thin Pb films have been observed by electron tunneling in early experiments by Lutsikii *et al.*²³

In this paper we present the differential conductance $G(V)$ for small contacts with a radius a smaller than the Fermi wavelength $\lambda_F = \hbar/p_F$, where p_F is the Fermi momentum. The contacts are formed on the surface of a thin metal film. Here we analyze the voltage dependence of $I(V)$ and $G(V)$. We focus on the size quantization effects of the electron energy spectrum in the film on $G(V)$.

The organization of this paper is as follows. The model that we use to describe the contact, and the method for obtaining a solution of the three-dimensional Schrödinger equation asymptotic in the small radius of the contact, are described in Sec. 2. In Sec. 3 the current-voltage characteristics and the differential conductance are found based on the calculation of the probability current density through the contact. Section 4 presents a physical interpretation of the results obtained. In Sec. 5 we conclude by discussing the possibilities for exploiting these theoretical results for the interpretation of electron energy spectroscopy in thin films by STM. In the Appendixes we solve the Schrödinger equation for the tunnel point contact in the framework of our model (Appendix 1) and for a point contact without a barrier (Appendix 2) and find the wavefunctions for electrons transmitted through the contact. These solutions are used in Sec. 3 for the calculation of current.

2. Model and electron wave function of the system

An illustration of the model under consideration is provided in Fig. 1. Electrons can tunnel through an orifice centered at point $\mathbf{r} = 0$ in an infinitely thin insulating interface at $z = 0$ from a conducting half-space (the tip) into a conducting sheet of thickness d (Fig. 1(b)). The radius a of the contact and the thickness d of the film are assumed to be much smaller than the shortest mean free path, i.e., we consider a purely ballistic problem. The wave function ψ satisfies the Schrödinger equation

$$\nabla^2 \psi(\mathbf{r}) + \frac{2m^*}{\hbar^2} [\varepsilon - U(\mathbf{r})] \psi(\mathbf{r}) = 0. \quad (1)$$

In Eq. (1) m^* and ε are the effective mass and energy of the electron, respectively. We describe the inhomogeneous potential barrier in the plane $z = 0$ by the function $U(\mathbf{r}) = U_0 f(\boldsymbol{\rho}) \delta(z)$, where $\boldsymbol{\rho} = (x, y)$ is a two-dimensional position vector in the plane z , and $f^{-1}(\boldsymbol{\rho}) = \Theta(a - \rho)$, where $\Theta(x)$ is the Heaviside step function. In such a model the wavefunction

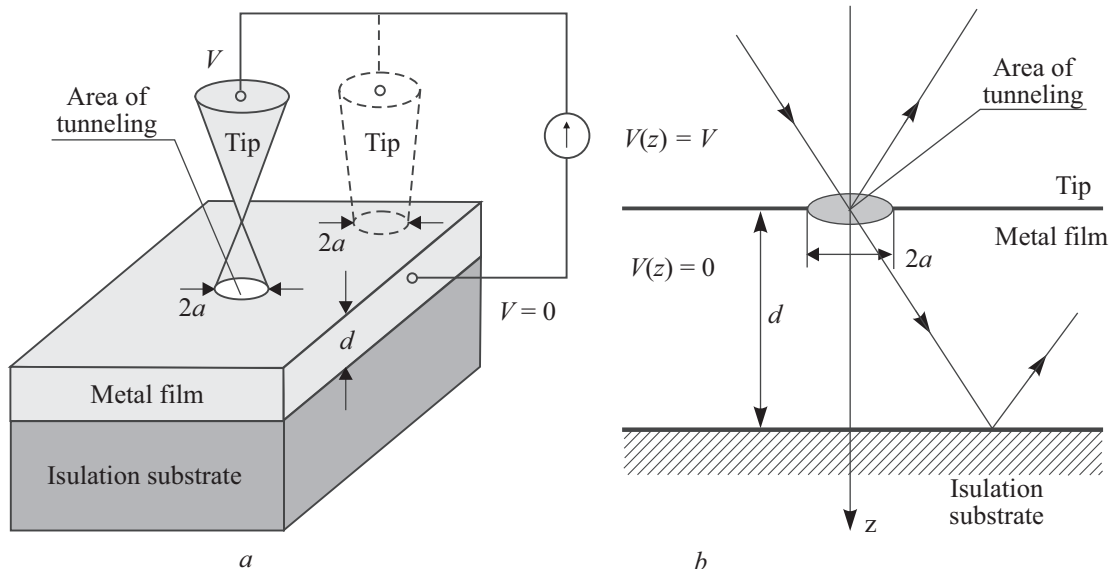


FIG. 1. Schematic representation of an STM experiment on a thin metal film (a) and the model that we employ to represent the contact between a bulk conductor (tip) and a metallic film (b). The dashed picture of the tip in (a) illustrates a metallic point contact (STM tip touches the surface). Electron trajectories in (b) are shown schematically.

$\psi(\mathbf{r})$ satisfies the following boundary conditions at the interface $z = 0$ and at the metal sheet surface $z = d$

$$\psi(\boldsymbol{\rho}, +0) = \psi(\boldsymbol{\rho}, -0), \quad (2)$$

$$\psi'_z(\boldsymbol{\rho}, +0) - \psi'_z(\boldsymbol{\rho}, -0) = \frac{2m^*U_0}{\hbar^2}f(\boldsymbol{\rho})\psi(\boldsymbol{\rho}, 0), \quad (3)$$

$$\psi(\boldsymbol{\rho}, d) = 0. \quad (4)$$

Equations (1)–(4) can be solved in the limit of a small contact, $ka \ll 1$ ($k = \sqrt{2m^*\varepsilon}/\hbar$ is the absolute value of the electron wave vector \mathbf{k}). In the contact diameter in the zeroth approximation the solutions of Eq. (1) for $z \geq 0$ are independent and satisfy the zero boundary condition $\psi(\boldsymbol{\rho}, 0) = 0$ at the impenetrable interface at $z = 0$. The quantum states in the conducting half-space ($z < 0$) (the tip) are defined by the three components of the electron wave vector $\mathbf{k} = (\mathbf{k}_{\parallel}, k_z)$, where \mathbf{k}_{\parallel} is a two-dimensional vector parallel to the interface. In the metal film ($0 < z < d$) the quantum states are characterized by a two-dimensional vector κ that is perpendicular to the z axis, and by the discrete quantum number n ($n = 1, 2, \dots$) resultant from the finite size of the conductor in the z direction. The energy eigenvalues and eigenfunctions for the two disconnected conductors are given by

$$\varepsilon = \frac{\hbar^2(k_{\parallel}^2 + k_z^2)}{2m^*} \equiv \frac{\hbar^2 k^2}{2m^*}, \quad (5)$$

$$\psi_0(\mathbf{r}) = 2ie^{i\mathbf{k}_{\parallel}\boldsymbol{\rho}} \sin k_z z, \quad z < 0, \quad (6)$$

and

$$\varepsilon = \frac{\hbar^2(\kappa^2 + k_{zn}^2)}{2m^*}, \quad n = 1, 2, \dots, \quad (7)$$

$$\psi_0(\mathbf{r}) = -2ie^{i\kappa\boldsymbol{\rho}} \sin k_{zn} z, \quad 0 < z < d, \quad (8)$$

where $k_{zn} = \pi n/d$. In Eqs. (6) and (8) we use wavefunction normalization with unit amplitude of the wave incident to the interface.

The partial wave for the first order approximation $\psi_1(\mathbf{r})$ in the small parameter $ka \ll 1$, which describes the transition of electrons from one to the other conductor, is given in the Appendix. In Appendix 1 Eqs. (A1.5) and (A1.6) give the solution for a tunnel point contact, having a potential barrier of small transparency $t = k\hbar^2/m^*U_0 \ll 1$ at the orifice in plane $z = 0$. In Appendix 2 Eqs. (A2.6)–(A2.8) give solutions for a contact without a barrier. Fig. 2 illustrates the spatial variation of the square modulus of the wavefunction for electrons transmitted through the contact into the film.

3. Current–voltage characteristic and conductance of a point contact

As previously shown,²⁴ for a ballistic point contact of small radius a , where a is much smaller than the electron mean free path l , the electrical potential $V(\mathbf{r})$ drops over distance $r \sim a$ from the contact, and in the limit $a \rightarrow 0$ the potential $V(\mathbf{r})$ can be approximated by a step function $V\Theta(-z)$. In this approximation, to calculate electrical current we can take the functions of electron distribution $f^{(\mp)}$ at $z \lesssim 0$ as the Fermi functions f_F with energies shifted by the

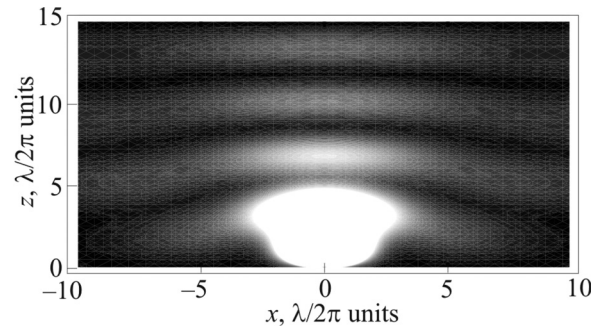


FIG. 2. Space distribution of the square modulus of the wave function for electrons injected by an STM tip into a metal sheet of thickness $d = 15$, where $\lambda = 2\pi/k$ is the electron wave length, $\hat{x} = \lambda/2\pi$.

applied bias eV (where e is the negative electron charge), $f^{(\mp)} = f_F(\varepsilon - eV\Theta(-z))$. Figure 3 illustrates the occupied energy states in the two conductors for both signs of the applied bias eV . At $eV > 0$ the electrons flow from the bulk conductor (the tip) into the film, and vice-versa: at $eV < 0$ they flow from the film into the bulk of the conductor. The total current through the area of the contact can be found by integration over the flux $J^{(\pm)}$ in both directions

$$I(V) = \frac{1}{2\pi d} \int_{-\infty}^{\infty} d\kappa \sum_{n=1}^{\infty} J^{(-)} f_F(\varepsilon)(1 - f_F(\varepsilon - eV)) - \frac{2}{(2\pi)^3} \int_{-\infty}^{\infty} d\mathbf{k} J^{(+)} f_F(\varepsilon - eV)(1 - f_F(\varepsilon)). \quad (9)$$

In Eq. (9) in the second term we integrate the wave vector \mathbf{k} in the semi-infinite conductor to represent the current in the negative direction, and in the first term we integrate the two-dimensional wave vector κ and the flux sum over the discrete quantum number n for the opposite direction of current.

For simplicity we choose the temperature to be zero. In this case the electric current is defined by electrons passing through the contact in one direction only, depending on the sign of the applied bias. The flux $J^{(\pm)}$ integrated over the area of the contact is calculated in the usual way

$$J^{(\pm)} = \frac{|e|\hbar}{m^*} \int_0^a d\rho \rho \int_0^{2\pi} d\varphi \text{Im} \left[\psi_1^*(\boldsymbol{\rho}, z) \frac{\partial}{\partial z} \psi_1(\boldsymbol{\rho}, z) \right]_{z=\pm 0}, \quad (10)$$

where $\boldsymbol{\rho} = (\rho \cos \varphi, \rho \sin \varphi)$. The wavefunction $\psi_1(\boldsymbol{\rho}, z)$ represents the wave transmitted through the contact given by Eqs. (A1.5) and (A2.6) with $\mathbf{k} = k_z$ for electron flux from the tip to the sheet, $J^{(+)}$, and by Eqs. (A1.6) and (A2.7) with $\mathbf{k} = k_{zn}$ ($n = 1, 2, \dots$) for fluxes $J^{(-)}$ in the opposite direction. The energy shift eV in the region $z < 0$ should be taken into account, which for the chosen energy reference point (see Fig. 3) implies that the absolute value of the electron wave vector in the half-space $z < 0$ is given by $\tilde{k} = \sqrt{2m^*(\varepsilon - eV)}/\hbar$.

For the tunnel point contact (tpc) the flux can be expressed in terms of the wavefunction in the contact plane (A1.1), and we obtain

$$J_{tpc}^{(+)} \simeq \frac{\pi^4 |e| a^4 \hbar^5 \tilde{k}^2 \cos^2 \vartheta}{12m^{*3} d^3 U_0^2} N(N+1)(2N+1) \quad (11)$$

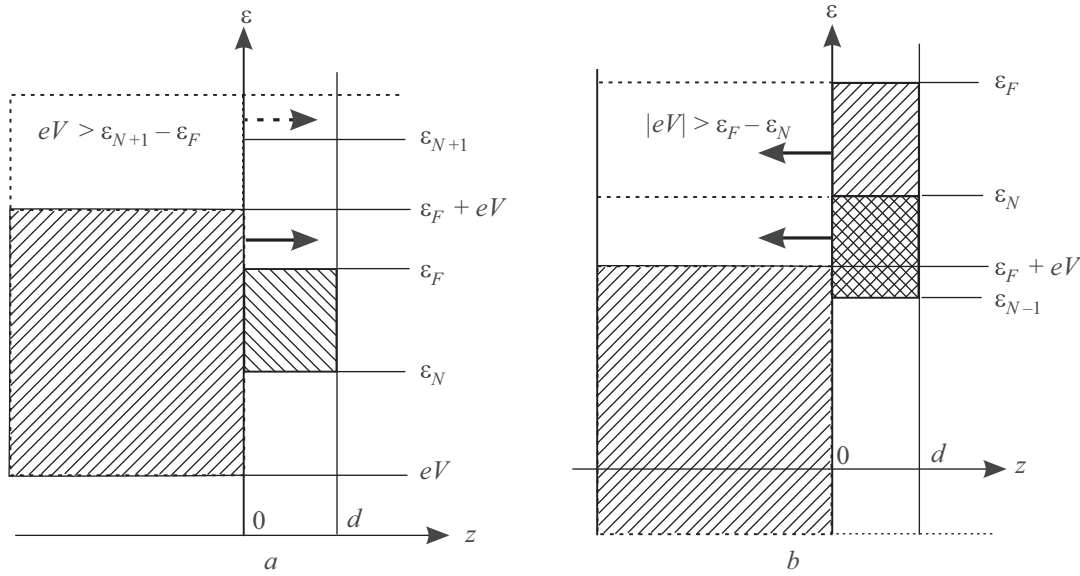


FIG. 3. Illustration of the occupied energy states at zero temperature in the two conductors for both signs of applied bias eV : $eV > 0$ (a), $eV < 0$ (b).

and

$$J_{tpc}^{(-)} \simeq -\frac{\pi|e|a^4\hbar^5\tilde{k}^3k_{zn}^2}{6m^*3U_0^2}. \quad (12)$$

Here, ϑ is the angle between the vector \mathbf{k} and the z -axis, and $N(k) = [kd/\pi]$, where $[x]$ is the integer part of x .

For a metallic point contact (mpc) without a barrier the expressions for the flux $J_{mpc}^{(\pm)}$ can be written using Eqs. (A2.4) and (A2.9)–(A2.11),

$$J_{mpc}^{(+)} \simeq \frac{\pi^2|e|\hbar a^6\tilde{k}^2\cos^2\vartheta}{9m^*d^3}N(N+1)(2N+1) \quad (13)$$

and

$$J_{mpc}^{(-)} \simeq -\frac{8\pi|e|\hbar a^6\tilde{k}^3k_{zn}^2}{9m^*}. \quad (14)$$

Substituting Eqs. (11)–(14) into the general expression (9) we determine the current–voltage characteristic of the system

$$I(V) = \frac{I_0}{(k_F d)^3} \int_{k_F}^{\tilde{k}_F} \frac{dkk^2}{k_F^5} \left(k^2 - \frac{2meV}{\hbar^2} \right) S_2(k), \quad eV \geq 0 \quad (15)$$

and

$$\begin{aligned} I(V) = & -\frac{I_0}{(k_F d)^3} \left\{ S_2(k_F) \left[\frac{1}{5} + \frac{2|eV|}{3\varepsilon_F} + \frac{1}{3} \left(\frac{|eV|}{\varepsilon_F} \right)^2 \right] \right. \\ & + [S_3(\tilde{k}_F) - S_3(k_F)] \frac{\pi}{k_F d} \left(\frac{|eV|}{\varepsilon_F} \right)^2 \\ & + \frac{2}{3} [S_5(\tilde{k}_F) - S_5(k_F)] \left(\frac{\pi}{k_F d} \right)^3 \frac{|eV|}{\varepsilon_F} \\ & + \frac{1}{5} [S_7(\tilde{k}_F) - S_7(k_F)] \left(\frac{\pi}{k_F d} \right)^5 \\ & \left. - S_2(\tilde{k}_F) \frac{\tilde{k}_F}{5k_F} \left[1 + \frac{4|eV|}{3\varepsilon_F} - \frac{8}{3} \left(\frac{|eV|}{\varepsilon_F} \right)^2 \right] \right\}, \quad eV \leq 0, \end{aligned} \quad (16)$$

where $\varepsilon_F = \hbar^2 k_F^2 / 2m^*$ is the Fermi energy,

$$I_{0,tpc} = \frac{|e|\pi^2 a^4 \hbar^5 k_F^8}{12m^*3U_0^2}, \quad (17)$$

$$I_{0,mpc} = \frac{e\hbar a^6 k_F^8}{9m^*}, \quad (18)$$

$S_m(k)$ is a finite sum of the m th powers of integers

$$S_m(k) = \sum_{n=1}^{N(k)} n^m. \quad (19)$$

Note that $S_m(k) \equiv H_{-m}(N)$, where $H_m(n)$ are the generalized harmonic numbers. The current is plotted in Fig. 4 as a function of bias voltage for two different film thicknesses. Differentiating Eqs. (15) and (16) with respect to voltage we obtain the differential conductance $G(V) = dI/dV$ for a point contact with radius $a \ll \lambda_F$,

$$G(V) = G_1 \left\{ \frac{\tilde{k}_F}{2k_F} S_2(\tilde{k}_F) - \frac{1}{k_F^3} \int_{k_F}^{\tilde{k}_F} dk k^2 S_2(k) \right\}, \quad eV \geq 0, \quad (20)$$

$$\begin{aligned} G(V) = & G_1 \left\{ \frac{4}{3} \left[1 + \frac{|eV|}{\varepsilon_F} \right] S_2(k_F) + 4 \frac{|eV|}{\varepsilon_F} \frac{\pi}{k_F d} \right. \\ & \times [S_3(\tilde{k}_F) - S_3(k_F)] + \frac{4}{3} \left(\frac{\pi}{k_F d} \right)^3 [S_5(\tilde{k}_F) - S_5(k_F)] \\ & \left. - \frac{k_F}{3\tilde{k}_F} \left[1 + 4 \frac{|eV|}{\varepsilon_F} - 8 \left(\frac{|eV|}{\varepsilon_F} \right)^2 \right] S_2(\tilde{k}_F) \right\}, \quad eV \leq 0. \end{aligned} \quad (21)$$

In the limit $eV \rightarrow 0$ the zero-bias conductance taken from both sides coincides, as it should,

$$G(0) = G_1 S_2(k_F) = \frac{G_1}{6} N_F(N_F + 1)(2N_F + 1), \quad (22)$$

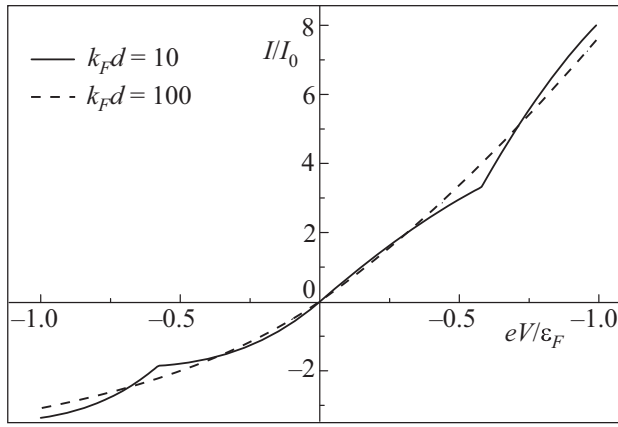


FIG. 4. Dependence of the total current, $I(V)$, on the applied bias over the point contact for two values of metal film thickness. The constant I_0 is given by Eqs. (17) or (18).

where $N_F = N(k_F)$, and G_1 is the conductance of the contact between the bulk conductor (the tip) and a thin film that has only a single energy level available below ε_F for the motion along z ,

$$G_1 = G_0(0) \frac{3\pi^3}{(k_F d)^3}. \quad (23)$$

$G_0(0)$ is the conductance of a contact between two conducting unbound half-spaces. For a tunnel point contact this is given by^{7,12}

$$G_{0,tpc}(0) = \left(\frac{k_F \hbar^2}{m^* U_0} \right)^2 \frac{e^2 (k_F a)^4}{36\pi \hbar}, \quad (24)$$

and for a metallic point contact we have²⁵

$$G_{0,mpc}(0) = \frac{8e^2 (k_F a)^6}{27\pi^3 \hbar}. \quad (25)$$

For $d \rightarrow \infty$ Eqs. (20) and (21) transform into the known voltage dependence of the conductance for a point contact between unbound conducting half-spaces,²⁷

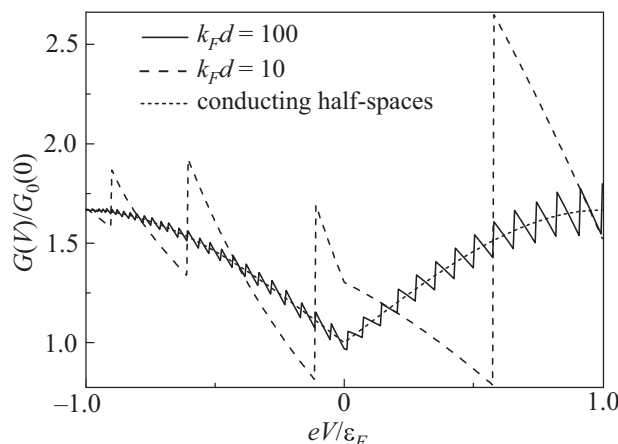


FIG. 5. Dependence of the normalized differential conductance, $G(V)/G_0(0)$, on the applied bias over the point contact for two values of metal film thickness. The voltage dependence for a point contact between two semi-infinite bulk conductors is shown for comparison (short-dashed curve).

$$G_0(V) = G_0(0) \left[1 + \frac{|eV|}{\varepsilon_F} - \frac{1}{3} \left(\frac{|eV|}{\varepsilon_F} \right)^3 \right]. \quad (26)$$

The dependence of the differential conductance $G(V)$ for both signs of applied voltage is illustrated in Fig. 5. For comparison, the dependence of $G_0(V)/G_0(0)$ from Eq. (26) is shown also.

4. Discussion

Thus, in the framework of the model illustrated in Fig. 1 we have obtained the current–voltage characteristic and the differential conductance for a contact on the surface of a thin metal film. Under the assumption that the contact radius a is much smaller than the Fermi wavelength λ_F we found asymptotically exact formulas for the dependence of the total current $I(V)$ (Eqs. (15) and (16)) and the contact conductance $G(V)$ (Eqs. (20) and (21)) on the applied voltage. In the limit of zero temperature and neglecting scattering processes we have demonstrated that the dependence $I(V)$ has kinks, and $G(V)$ exhibits jumps at the same values of applied bias eV (see Figs. 4 and 5). These events result from the size quantization of the electron spectrum in the film.

The results obtained show that even in Ohm's-law approximation (22), $eV \rightarrow 0$, the conductance $G(V)$ is not simply proportional to the electron density of states (DOS) in the isolated film,

$$\rho_f(\varepsilon) = \frac{m^* N_F}{\pi \hbar^2 d}. \quad (27)$$

It is remarkable that the dependence of conductance $G(0)$ (Eq. (22)) on the number of quantum levels N_F is the same for both the tunnel and the metallic point contacts. This fact proves that such dependence is not sensitive to the model taken for the potential barrier, and that it is the result of point-contact geometry. Recently, the relationship between the differential conductance and the local density of states has been studied in a tight-binding approximation for tunnel junctions, where the junction geometry can be varied between the limiting cases of a point-contact and a planar junction.²⁸ In the framework of real-space Keldysh formalism the authors of Ref. 28 have shown that the differential conductance is not, in general, proportional to the DOS of the sample for planar junctions, although features of the DOS may be present.

From Eqs. (20) and (21) it follows that the conductance is nonsymmetric in the applied bias. This asymmetry can be explained as follows: Let $eV > 0$ and electrons tunnel from the bulk conductor into the film (Fig. 3(a)), in which N_F subbands of the size quantization are partially filled. If the bias eV is smaller than the distance $\Delta\varepsilon$ between the Fermi level ε_F and the bottom of the next (empty) subband $\varepsilon_{N+1} = \pi^2 \hbar^2 (N_F + 1)^2 / 2m^* d^2$, $\Delta\varepsilon = \varepsilon_{N+1} - \varepsilon_F$, the electron can tunnel into any of the N_F subbands. At $eV = \Delta\varepsilon$ tunneling into the $(N_F + 1)$ -th subband becomes possible, and the conductance $G(V)$ undergoes a positive jump. Such jumps are repeated with increasing voltage for all higher subbands. For $eV < 0$, when electrons tunnel from the thin film into bulk metal (Fig. 3(b)) the situation is somewhat different. If the bias $|eV|$ becomes larger than distance $\Delta\varepsilon$ between the bottom of

the last partially filled subband $\varepsilon_N = \pi^2 \hbar^2 N_F^2 / 2m^* d^2$ and the Fermi energy, $\Delta\varepsilon = \varepsilon_F - \varepsilon_N$, the contribution of the N_F -th subband to the tunnel current does not depend on the voltage because for any $|eV| > \Delta\varepsilon$ all the electrons of this subband can tunnel into the bulk states of the left conductor. For this reason the differential conductance drops for values of $|eV|$ that coincide with the bottom of size quantization subbands in the film. The distance between the neighboring jumps of conductance on the voltage scale equals the distance between energy levels $\Delta\varepsilon_N = \varepsilon_{N+1} - \varepsilon_N = \pi^2 \hbar^2 (2N_F + 1) / 2m^* d^2$. For $eV < 0$ the number of conductance jumps is finite and equals the number of discrete levels below the Fermi surface N_F . The asymmetry around $V=0$ and the general shape of the jumps in the conductance can be recognized in the experiments, e.g., see Ref. 15. In the special case of a 2D electron system, which has only one level in the potential well, there is a single negative jump of $G(V)$. Such a jump was observed in Ref. 29 by STM investigations of the 2D electron gas at noble-metal surfaces. For $eV > 0$ the number of conductance jumps formally is not restricted. However, for $eV > \varepsilon_F$ our approach is no longer applicable, and the influence of field emission on the tunnel current must be taken into account.^{30,31}

The observation of manifestations of the size quantization in the STM conductance requires a few conditions to be fulfilled: the distance between the energy levels must be large enough and should satisfy the condition $\Delta\varepsilon_N \gg \hbar/\tau, T$, where τ is the mean scattering time of the electrons in the film, and T is the temperature. The surfaces of the metal film in the region of the contact must be atomically smooth.³² When the finite lifetime of the quantized states becomes relevant, the temperature broadening of the Fermi function, or surface imperfections, need to be taken into account. This will result in a rounding of the jumps in the curve $G(V)$ presented in Fig. 5 (Eqs. (20) and (21)), which was plotted under assumptions of perfectly specular surfaces, $T=0$, and $\tau \rightarrow \infty$. With these restrictions taken into account the current–voltage curves in Fig. 4 give a fair qualitative description of the experimental results of Ref. 14.

It can be easily seen that for the conducting film the results obtained have a wider domain of applicability than that of a rectangular well. For any model of potential that restricts the electron motion in one direction the differential conductance has a step-like dependence on the applied bias with distances between the steps equal to the distances between the quantum levels.

5. Conclusion

In summary, we have investigated the conductance of ultrasmall contacts, the radius of which is smaller than the Fermi wavelength, on the surface of a thin film. The discreteness of the component of electron momentum that is transverse to the film surface is taken into account. The distance between the electron energy levels is assumed to be larger than the temperature due to size quantization. Both, a contact with a potential barrier of low transparency and a contact without a barrier have been considered. In the framework of our model we obtained the current–voltage characteristic $I(V)$ of the system and the differential conductance $G(V)$ using a δ -function potential barrier. We predict a sawtooth

dependence of $G(V)$ on the applied bias and show that the distance between neighboring jumps is equal to the distance between neighboring energy levels of size quantization, i.e., this dependence can be used for spectroscopy of size quantized levels. At $eV > 0$ the jumps in the conductance are positive and correspond to distances between the levels found above the Fermi surface, while $G(V)$ undergoes negative jumps for $eV < 0$, the distances between which are equal to the distances between the levels below the Fermi surface. The predicted quantization of conductance can be observed in STS experiments, and the shape of theoretical curves agrees with experiments well.

Appendix 1: Electron tunneling between the tip and the thin film

We look for a solution to Eq. (1) at $V=0$ in the form of a sum $\psi = \psi_0 + \psi_1$ for the incident and backscattered waves, and $\psi = \psi_1$ for the transmitted wave. Here, ψ_0 , as given by Eqs. (6) and (8), is the unperturbed wave function that does not depend on the barrier amplitude U_0 , while $\psi_1 \sim 1/U_0$ gives the first order correction. Substituting the wave function into the boundary conditions (2) and (3) one should match the terms of the same order in $1/U_0$. As a result, boundary condition (3) becomes⁷

$$\psi_1(\boldsymbol{\rho}, 0) = -\frac{i\mathbb{k}\hbar^2}{m^*U_0} e^{i\boldsymbol{\kappa}\boldsymbol{\rho}} \Theta(a - \rho), \quad (\text{A1.1})$$

where $\mathbb{k} = k_z$ when the wave is incident to the contact from the tip side, and $\mathbb{k} = k_{zn}$ when the wave arrives at the contact from the sheet. For $ka \ll 1$ we have $\boldsymbol{\kappa}\boldsymbol{\rho} \ll 1$ in the plane of the contact, and we can neglect the exponent in the boundary condition (A1.1).

The function $\psi_1(\boldsymbol{\rho}, z)$ can be represented as a Fourier integral

$$\psi_1(\boldsymbol{\rho}, z) = \int_{-\infty}^{\infty} d\boldsymbol{\kappa}' e^{-i\boldsymbol{\kappa}'\boldsymbol{\rho}} \Psi(\boldsymbol{\kappa}', z). \quad (\text{A1.2})$$

The Fourier components in Eq. (A1.2) should satisfy the zero boundary condition at $z=d$, but are otherwise freely propagating along z ,

$$\Psi(\boldsymbol{\kappa}', z) = \Psi(\boldsymbol{\kappa}', 0) \frac{\sin k'_z(z-d)}{\sin k'_z d}, \quad 0 \leq z \leq d, \quad (\text{A1.3})$$

$$\Psi(\boldsymbol{\kappa}', z) = \Psi(\boldsymbol{\kappa}', 0) \exp(-ik'_z z), \quad z \leq 0, \quad (\text{A1.4})$$

with $k'_z = \sqrt{k^2 - \boldsymbol{\kappa}'^2}$, $k = \sqrt{2m^*\varepsilon}/\hbar$. From Eqs. (A1.1) and (A1.2) it follows that

$$\Psi(\boldsymbol{\kappa}', 0) = \frac{1}{(2\pi)^2} \int_{-\infty}^{\infty} d\boldsymbol{\rho} e^{i\boldsymbol{\kappa}'\boldsymbol{\rho}} \psi(\boldsymbol{\rho}, 0) = -\frac{i\mathbb{k}\hbar^2 a}{2\pi m^* U_0} \frac{J_1(\boldsymbol{\kappa}' a)}{\boldsymbol{\kappa}'}. \quad (\text{A1.5})$$

Substituting this into Eq. (A1.2) we find the wavefunctions for the electrons transmitted through the contact as

$$\Psi_1(\rho, z) = \frac{i\mathbb{k}\hbar^2 a}{m^* U_0} \int_0^\infty d\kappa' J_0(\kappa' \rho) J_1(\kappa' a) \frac{\sin \kappa'_z (d-z)}{\sin \kappa'_z d},$$

$$0 < z \leq d, \quad (\text{A1.6})$$

$$\Psi_1(\rho, z) = \frac{i\mathbb{k}\hbar^2 a}{m^* U_0} \int_0^\infty d\kappa' J_0(\kappa' \rho) J_1(\kappa' a) \exp(-i\kappa'_z z),$$

$$z < 0, \quad (\text{A1.7})$$

where $J_n(x)$ is the Bessel function of the first kind.

Appendix 2: Metallic point contact between STM tip and metal film

Here we consider a point contact without a potential barrier in the plane of the interface. When the contact radius is small, $ka \ll 1$, we can use perturbation theory for the electron wavefunction in the limit $a \rightarrow 0$. In the zeroth approximation the wavefunctions are given by Eqs. (6) and (8). The first order correction, $\psi_1(\rho, 0)$, to the wave function in the plane of the contact can be found by the method proposed in Ref. 25. For distances $r \ll \lambda$ from the contact we can neglect the second term in the Schrödinger equation (1), and it reduces to the Laplace equation. We express the wavefunction in coordinates of an oblate ellipsoid of revolution (σ, τ, φ), with $\sigma \geq 0$ and $-1 \leq \tau \leq 1$. As a consequence of the cylindrical symmetry of the problem the wavefunction $\psi_1(\sigma, \tau)$ does not depend on φ . The interface corresponds to $\tau=0$ and the plane of the orifice is at $\sigma=0$. In these coordinates we obtain the equation

$$\frac{\partial}{\partial \sigma} \left[(1 + \sigma^2) \frac{\partial \Psi_1}{\partial \sigma} \right] + \frac{\partial}{\partial \tau} \left[(1 - \tau^2) \frac{\partial \Psi_1}{\partial \tau} \right] = 0, \quad (\text{A2.1})$$

with the boundary condition at the interface

$$\psi_1(\sigma > 0, \tau = 0) = 0. \quad (\text{A2.2})$$

The solution of the boundary problem (A2.1) and (A2.2) is

$$\psi_1(\sigma, \tau) = \tau [c_1 \sigma + c_2 (1 + \sigma \arctan \sigma)], \quad (\text{A2.3})$$

where c_1 and c_2 are constants. For $\sigma=0$ Eq. (A2.3) gives the function $\psi_1(\rho, z)$ in the plane of the contact $z=0, \rho \leq a$

$$\psi_1(\rho, 0) = c_2 \sqrt{1 - \frac{\rho^2}{a^2}}. \quad (\text{A2.4})$$

As in Appendix 1, we express $\psi_1(\rho, z)$ as a Fourier integral and, using Eq. (A2.4), we find for the Fourier components

$$\Psi(\kappa', 0) = \frac{1}{(2\pi)^2} \int_{-\infty}^\infty d\rho e^{i\kappa' \rho} \psi_1(\rho, 0) = c_2 a \frac{j_1(\kappa' a)}{\kappa'}, \quad (\text{A2.5})$$

where $j_1(x)$ is the spherical Bessel function of the first kind. Substituting Eqs. (A2.5) into (A1.2) and using Eqs. (A1.3) and (A1.4) we obtain

$$\psi_1(\rho, z) = \frac{c_2 a}{2\pi} \int_0^\infty d\kappa' J_0(\kappa' \rho) j_1(\kappa' a) \frac{\sin \kappa'_z (d-z)}{\sin \kappa'_z d}.$$

$$0 < z \leq d, \quad (\text{A2.6})$$

and

$$\psi_1(\rho, z) = \frac{c_2 a}{2\pi} \int_0^\infty d\kappa' J_0(\kappa' \rho) j_1(\kappa' a) e^{-i\kappa'_z z}, \quad z < 0. \quad (\text{A2.7})$$

The constant c_2 must be found from the boundary condition (3) at $U_0=0$, which for this case takes the form

$$\frac{\partial \psi_1(\rho, +0)}{\partial z} - \frac{\partial \psi_1(\rho, +0)}{\partial z} - 2i\mathbb{k} = 0. \quad (\text{A2.8})$$

The meaning of the symbol \mathbb{k} is explained below Eq. (A1.1). Differentiating Eqs. (A2.6) and (A2.7) with respect to z and calculating the integrals in the limit of small a we find

$$\frac{\partial \psi_1}{\partial z} \Big|_{z=+0} \simeq \frac{c_2 a}{2\pi} \left[-\frac{\pi}{2a^2} + i \frac{\pi^3 a}{18d^3} N(N+1)(2N+1) \right], \quad (\text{A2.9})$$

$$\frac{\partial \psi_1}{\partial z} \Big|_{z=-0} \simeq \frac{c_2 a}{2\pi} \left(\frac{\pi}{2a^2} + i \frac{\pi k^3 a}{9} \right), \quad (\text{A2.10})$$

where $N = [kd/\pi]$, and $[x]$ is the integer part of x . Substituting Eqs. (A2.9) and (A2.10) into Eq. (A2.8) in the leading approximation in a , in which only the first terms in the brackets (proportional to $1/a^2$) should be taken into account, for the unknown constant we find

$$c_2 \simeq 2i\mathbb{k}a. \quad (\text{A2.11})$$

^{a)}Email: khotkevych@ilt.kharkov.ua

¹W. A. Hofer, A. S. Foster, and A. L. Shluger, *Rev. Mod. Phys.* **75**, 1287 (2003).
²J. M. Blanco, F. Flores, and R. Pérez, *Prog. Surf. Sci.* **81**, 403 (2006).
³J. Tersoff and D. Hamann, *Phys. Rev. Lett.* **50**, 1998 (1983); *Phys. Rev. B* **31**, 805 (1985).
⁴J. Bardeen, *Phys. Rev. Lett.* **6**, 57 (1961).
⁵K. Kobayashi, *Phys. Rev. B* **53**, 11091 (1996).
⁶Ye. S. Avotina, Yu. A. Kolesnichenko, A. N. Omelyanchouk, A. F. Otte, and J. M. van Ruitenbeek, *Phys. Rev. B* **71**, 115430 (2005).
⁷I. O. Kulik, Yu. N. Mitsai, and A. N. Omelyanchouk, *Zh. Eksp. Teor. Fiz.* **66**, 1051 (1974).
⁸Ye. S. Avotina, Yu. A. Kolesnichenko, A. F. Otte, and J. M. Ruitenbeek, *Phys. Rev. B* **74**, 085411 (2006).
⁹Ye. S. Avotina, Yu. A. Kolesnichenko, S. B. Roobol, and J. M. Ruitenbeek, *Fiz. Nizk. Temp.* **34**, 268 (2008) [*Low Temp. Phys.* **34**, 207 (2008)].
¹⁰Ye. S. Avotina, Yu. A. Kolesnichenko, A. F. Otte, and J. M. Ruitenbeek, *Phys. Rev. B* **75**, 125411 (2007).
¹¹N. V. Khotkevych, Yu. A. Kolesnichenko, and J. M. van Ruitenbeek, *Fiz. Nizk. Temp.* **37**, 64 (2011) [*Low Temp. Phys.* **37**, 53 (2011)].
¹²Ye. S. Avotina, Yu. A. Kolesnichenko, and J. M. van Ruitenbeek, *Fiz. Nizk. Temp.* **36**, 1066 (2010) [*Low Temp. Phys.* **36**, 849 (2010)].
¹³I. B. Altfeder, K. A. Matveev, and D. M. Chen, *Phys. Rev. Lett.* **78**, 2815 (1997).
¹⁴I. B. Altfeder, D. M. Chen, and K. A. Matveev, *Phys. Rev. Lett.* **80**, 4895 (1998).

- ¹⁵C.-S. Jiang, H.-B. Yu, X.-D. Wang, C.-K. Shih, and Ph. Ebert, *Phys. Rev. B* **64**, 235410 (2001).
- ¹⁶W. B. Su, S. H. Chang, W. B. Jian, C. S. Chang, L. J. Chen, and T. T. Tsong, *Rev. Lett.* **86**, 5116 (2001).
- ¹⁷I. B. Altfeder, V. Narayanamurti, and D. M. Chen, *Phys. Rev. Lett.* **88**, 206801 (2002).
- ¹⁸H. Yu, C.-S. Jiang, Ph. Ebert, and C.-K. Shih, *Appl. Phys. Lett.* **81**, 2005 (2002).
- ¹⁹W. B. Jian, W. B. Su, C. S. Chang, and T. T. Tsong, *Phys. Rev. Lett.* **90**, 196603 (2003).
- ²⁰V. A. Gasparov, *Fiz. Nizk. Temp.* **37**, 1073 (2011) [*Low Temp. Phys.* **37**, 856 (2011)].
- ²¹L. C. Davis, R. C. Jaklevic, and J. Lambe, *Phys. Rev. B* **12**, 798 (1975).
- ²²A. I. Khachaturov, *J. Exp. Theor. Phys.* **91**, 541 (2000).
- ²³V. N. Lutskii, D. N. Korneev, and M. I. Elinson, *JETP Lett.* **4**, 179 (1966).
- ²⁴I. O. Kulik, A. N. Omel'anchuk, and R. I. Shekhter, *Fiz. Nizk. Temp.* **3**, 1543 (1977) [*Sov. J. Low Temp. Phys.* **3**, 740 (1977)].
- ²⁵I. F. Itskovich and R. I. Shekhter, *Fiz. Nizk. Temp.* **11**, 373 (1985) [*Sov. J. Low Temp. Phys.* **11**, 202 (1985)].
- ²⁶G. A. Korn and T. M. Korn, *Mathematical Handbook* (Dover, New York, 2000).
- ²⁷Ye. S. Avotina, Yu. A. Kolesnichenko, and J. M. Ruitenbeek, *J. Phys.: Condens. Matter* **20**, 115208 (2008).
- ²⁸C. Berthod and T. Giamarchi, *Phys. Rev. B* **84**, 155414 (2011).
- ²⁹L. Bürgi, N. Knorr, H. Brune, M. A. Schneider, and K. Kern, *Appl. Phys. A* **75**, 141 (2002).
- ³⁰O. Yu. Kolesnychenko, O. I. Shklyarevskii, and H. van Kempen, *Phys. Rev. Lett.* **83**, 2242 (1999).
- ³¹C. Pauly, M. Grob, M. Pezzotta, M. Pratzner, and M. Morgenstern, *Phys. Rev. B* **81**, 125446 (2010).
- ³²B. A. Tavger and V. Ya. Demikhovski, *Sov. Phys. Usp.* **11**, 644 (1969).

This article was published in English in the original Russian journal. Reproduced here with stylistic changes by AIP.